

Supporting information

A Low-cost Sulfate-based All Iron Flow Battery

Sicen Yu, Xiujun Yue, John Holoubek, Xing Xing, Eric Pan, Tod Pascal, Ping Liu*

Table S1. Viscosity and conductivity of electrolytes of interest.

	Viscosity (mPa·s)	Conductivity ($\mu\text{S cm}^{-1}$)
1 M FeSO₄	1.36±0.16	5278±28
1 M FeSO₄ with 0.1 M EMIC	1.63±0.38	5287±13
2 M FeSO₄ with 0.1 M EMIC	3.71±0.36	5468±17

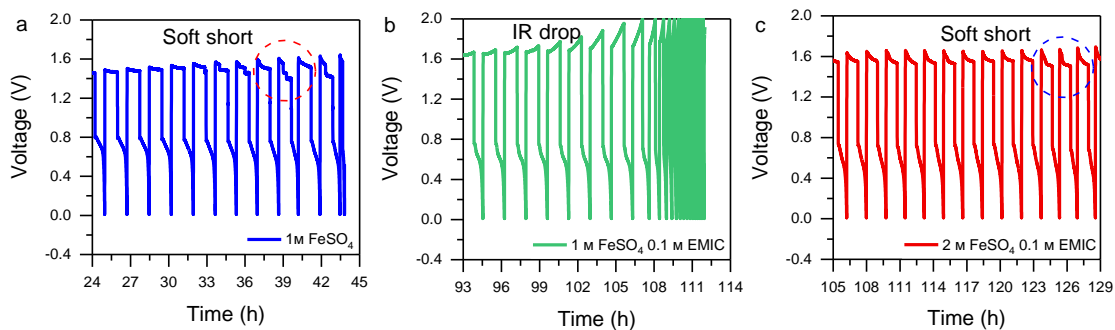


Fig. S1. The charge-discharge profiles of the FeSO₄-based AIFBs. The charge-discharge profiles in the final cycles prior to failure for the cells with (a) 1 M FeSO₄, (b) 1 M FeSO₄ with 0.1 M EMIC, and (c) 2 M FeSO₄ with 0.1 M EMIC electrolytes.

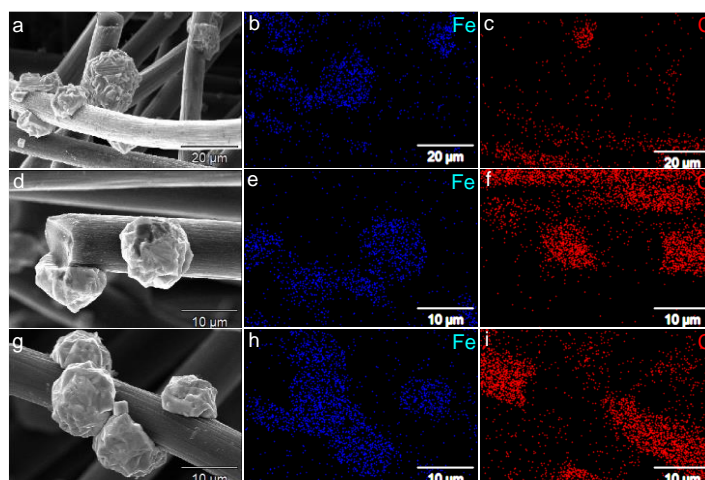


Fig. S2. Iron morphology in the FeSO₄-based AIFBs. Iron morphology in the carbon felt in (a)-(c) 1 M FeSO₄, (d)-(f) 1 M FeSO₄ with 0.1 M EMIC, and (g)-(i) 2 M FeSO₄ with 0.1 M EMIC electrolytes. All samples were fabricated at 20 mA/cm², one hour.

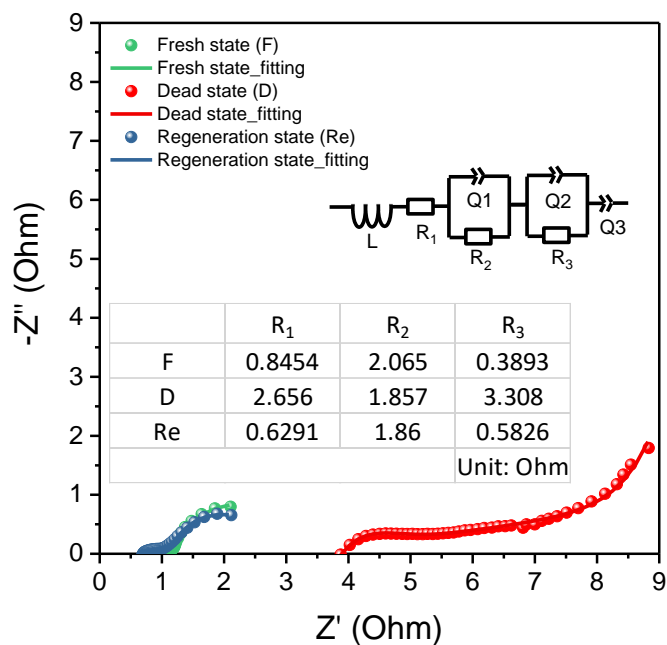


Fig. S3. EIS analysis of the FeSO_4 -based AIFBs. The EIS curves of flow battery with 2 M FeSO_4 with 0.1 M EMIC electrolytes at fresh state, dead state (discharged), and regenerated state. Embedded table exhibited the results of fitting circuit.

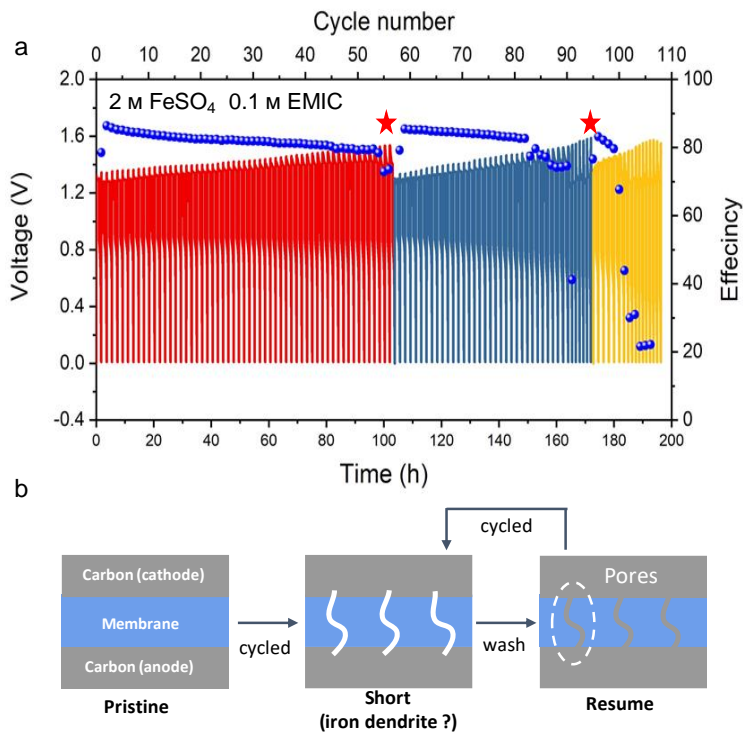


Fig. S4. The charge-discharge profiles of the FeSO_4 -based AIFBs with traditional set up. (a) Regeneration test with 2 M FeSO_4 with 0.1 M EMIC electrolyte, where red stars mean regeneration, and (b) schematic diagram of regeneration with traditional set up.

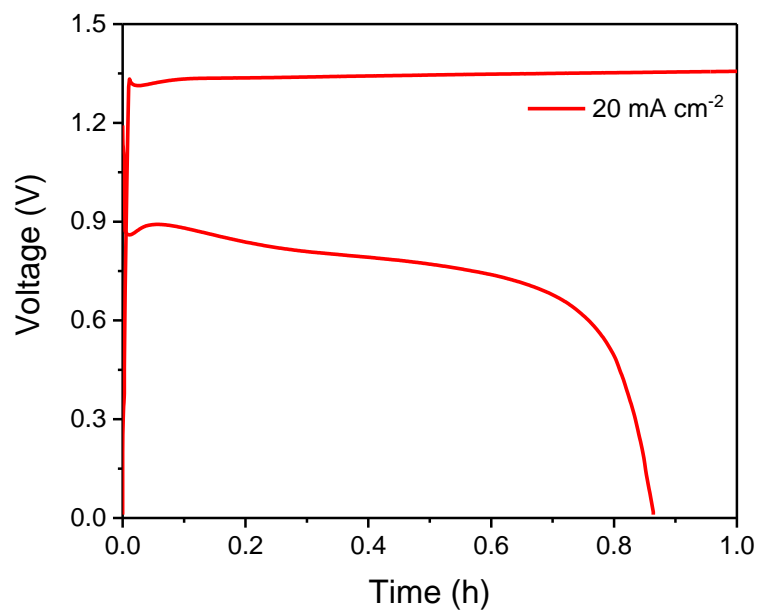


Fig. S5. The 156th cycle charge-discharge profile of the FeSO₄-based AIFBs with GF membrane (Fig. 5). The battery was run with 2 M FeSO₄ with 0.1 M EMIC electrolyte at a current density of 20 mA cm⁻².

Table S2. Flow batteries performance comparison

Ref	Iron salt	Main topic	membrane	Current density [mA cm ⁻²]	Capacity [mAh cm ⁻²]	Cycle number
[1]	FeCl ₂	Influence of electrolyte additives, temperature, and pH on improving the coulombic efficiency of the iron electrode.	No full-cell cycling performance.			
[2]	FeCl ₂	Ligands effects on stabilizing Fe(III) in aqueous solution.	No full-cell cycling performance.			
[3]	FeCl ₂	Iron electrodeposition in a deep eutectic solvent.	Daramic 175 microporous separator	5	5	16
[4]	FeCl ₂	Evaluation on full-cell cycling performance.	AEM (Tokuyama A901, 11 μm thickness)	40	3.3	50
[5]	FeCl ₂	MWCNT slurry electrode.	Not mentioned	75	0.5	12
[6]	FeCl ₂	Internal rebalancing system.	Daramic separator with PVA coating	100	100	<120
[7]	FeCl ₂ /FeSO ₄	Influence of supporting electrolytes on iron plating reaction.	No full-cell cycling performance.			
[8]	FeCl ₂ /FeSO ₄	Negative electrode engineering.	Daramic separator	40	20	6
[9]	Fe ₂ (SO ₄) ₃	Influence of Fe salts, separators, Fe electrodes, and supporting electrolytes on AIFB.	No full-cell cycling performance.			
[10]	FeSO ₄	Cost analysis.	No full-cell cycling performance.			
This work	FeSO ₄	High-concentration FeSO ₄ -based electrolyte.	Microporous membrane	20	20	>800

Table S3. Prices of the redox compounds

Chemical	Molecule weight [g mol ⁻¹]	Price [\$ kg ⁻¹]	n	Ur[\$ Ah ⁻¹]
V ₂ O ₅ ^{a)}	182	11.7	2	0.079
FeCl ₂ ^{b)}	126.75	0.086	1	0.00041
ZnCl ₂ ^{b)}	225.21	2.17	2	0.0091
FeSO ₄ 7H ₂ O (anode) ^{c)}	278.02	0.05	2	0.00026
FeSO ₄ 7H ₂ O (cathode) ^{c)}	278.02	0.05	1	0.00052

^{a)} Reference [11]; ^{b)} Reference[12]; ^{c)} Quoted from Shandong Jiulong Qingjiang Water Purification Technology Co., Ltd.

Table S4. Prices of supporting electrolytes

Chemical	Molecule weight [g mol ⁻¹]	Price [\$ kg ⁻¹]	Use [\$ Ah ⁻¹]
H ₂ SO ₄ ^{a)}	98	0.075	0.00099
KCl ^{b)}	74.45	0.26	0.0014

C₂H₅NO₂ ^{b)}	75.07	1.88	0.011
EMIC (anode) ^{c)}	146.62	1	0.00049
EMIC (cathode) ^{c)}	146.62	1	0.000985

^{a)} Reference [11]; ^{b)} Reference [12]; ^{c)} Quoted from Shanghai Yuchuang Chemical Technology Co., Ltd.

Table S5. Prices of electrode materials

Electrode material	Price [\$ m⁻²]	U_{em} [\$ m⁻²]
Carbon felt ^{a)}	70	70
Copper mesh ^{a)}	48	48
Carbon felt ^{b)}	154.7	154.7
Carbon felt ^{c)}	70	70

^{a)} Reference [11]; ^{b)} Reference [12]; ^{c)} Reference[13]

Table S6. Prices of the membranes

Membrane	Price [\$ m ⁻²]	U _m [\$ m ⁻²]
Nafion 117 cation-exchange membrane ^{a)}	500	500
PBI porous membrane ^{b)}	50	50
Microporous membrane ^{c)}	10	10
Glass fiber separator ^{d)}	0.1	0.1

^{a)} Reference [11]; ^{b)} Reference [12]; ^{c)} Reference [13]; ^{d)} Quoted from Qingdao Rockpro Composites Co., Ltd.

Table S7. Electrolyte costs of All-V, Zn-Fe, and FeSO₄/EMIC RFBs

	U _e [\$ Ah ⁻¹]	V _{eff} [V]	C _e [\$ kWh ⁻¹]
All-V ^{a)}	0.08064	1.26	64
Zn-Fe ^{b)}	0.021	1.4	15
FeSO ₄ /EMIC ^{c)}	0.00304	0.9	3.37

a) Reference [11]; b) Reference [12]; c) The price information and detailed calculation are shown in **Table S3** and **Table S4**.

Table S8. Stack costs of All-V, Zn-Fe RFBs and FeSO₄/EMIC.

	U_{em} [\$ m ⁻²]	U_m [\$ m ⁻²]	U_b [\$ m ⁻²]	U_s [\$ m ⁻²]
All-V ^{a)}	140	500	55	695
Zn-Fe ^{b)}	154.7	50	55	259.7
FeSO ₄ /EMIC ^{c)}	70	10.1	55	135.1

a) Reference [11]; b) Reference[12]; c) The price information and detailed calculation are shown in **Table S5**, and **Table S6**.

Table S9. Energy density analysis of All-V, Zn-Fe RFBs and FeSO₄/EMIC flow battery.

	V_{eff} [V]	Catholyte	Anolyte	Catholyte/Anolyte ratio [vol%]	Energy density [Wh L ⁻¹]
All-V ^{a)}	1.26	1.5 M VO ²⁺	1.5 M V ³⁺	1:1	25
Zn-Fe ^{b)}	1.4	2 M FeCl ₂	1 M ZnCl ₂	1:1	37

FeSO₄/EMIC ^{c)}	0.9	2 m FeSO ₄	2 m FeSO ₄	2:1	32
--	-----	-----------------------	-----------------------	-----	----

^{a)} Reference [11]; ^{b)} Reference[12]; ^{c)} This work.

Reference

- [1] B.S. Jayathilake, E.J. Plichta, M.A. Hendrickson, S.R. Narayanan, Improvements to the coulombic efficiency of the iron electrode for an all-iron redox-flow battery, *Journal of The Electrochemical Society*. 165 (2018) A1630.
- [2] K.L. Hawthorne, J.S. Wainright, R.F. Savinell, Studies of iron-ligand complexes for an all-iron flow battery application, *Journal of The Electrochemical Society*. 161 (2014) A1662–A1671.
- [3] M.A. Miller, J.S. Wainright, R.F. Savinell, Iron Electrodeposition in a Deep Eutectic Solvent for Flow Batteries, *Journal of The Electrochemical Society*. 164 (2017) A796–A803.
<https://doi.org/10.1149/2.1141704jes>.
- [4] A.K. Manohar, K.M. Kim, E. Plichta, M. Hendrickson, S. Rawlings, S.R. Narayanan, A high efficiency iron-chloride redox flow battery for large-scale energy storage, *Journal of The Electrochemical Society*. 163 (2015) A5118.
- [5] T.J. Petek, N.C. Hoyt, R.F. Savinell, J.S. Wainright, Slurry electrodes for iron plating in an all-iron flow battery, *Journal of Power Sources*. 294 (2015) 620–626.
<https://doi.org/10.1016/j.jpowsour.2015.06.050>.
- [6] S. Selverston, E. Nagelli, J.S. Wainright, R.F. Savinell, All-Iron Hybrid Flow Batteries with In-Tank Rebalancing, *Journal of The Electrochemical Society*. 166 (2019) A1725–A1731.
<https://doi.org/10.1149/2.0281910jes>.
- [7] K.L. Hawthorne, T.J. Petek, M.A. Miller, J.S. Wainright, R.F. Savinell, An investigation into factors affecting the iron plating reaction for an all-iron flow battery, *Journal of The Electrochemical Society*. 162 (2015) A108–A113.
- [8] K.L. Hawthorne, J.S. Wainright, R.F. Savinell, Maximizing plating density and efficiency for a negative deposition reaction in a flow battery, *Journal of Power Sources*. 269 (2014) 216–224.
<https://doi.org/10.1016/j.jpowsour.2014.06.125>.
- [9] M.C. Tucker, A. Phillips, A.Z. Weber, All-iron redox flow battery tailored for off-grid portable applications, *ChemSusChem*. 8 (2015) 3996–4004.
- [10] N. Yensen, P.B. Allen, Open source all-iron battery for renewable energy storage, *HardwareX*. 6 (2019) e00072. <https://doi.org/10.1016/j.ohx.2019.e00072>.
- [11] K. Gong, X. Ma, K.M. Conforti, K.J. Kuttler, J.B. Grunewald, K.L. Yeager, M.Z. Bazant, S. Gu, Y. Yan, A zinc–iron redox-flow battery under \$100 per kW h of system capital cost, *Energy & Environmental Science*. 8 (2015) 2941–2945. <https://doi.org/10.1039/c5ee02315g>.
- [12] C. Xie, Y. Duan, W. Xu, H. Zhang, X. Li, A Low-Cost Neutral Zinc–Iron Flow Battery with High Energy Density for Stationary Energy Storage, *Angewandte Chemie International Edition*. 56 (2017) 14953–14957.
- [13] V. Viswanathan, A. Crawford, D. Stephenson, S. Kim, W. Wang, B. Li, G. Coffey, E. Thomsen, G. Graff, P. Balducci, Cost and performance model for redox flow batteries, *Journal of Power Sources*. 247 (2014) 1040–1051.